Irrig Sci (2006) 24: 233–240
DOI 10.1007/s00271-005-0022-8

ORIGINAL PAPER

M. P. González-Dugo · M. S. Moran · L. Mateos
R. Bryant

Canopy temperature variability as an indicator of crop water stress severity

Received: 9 February 2005 / Accepted: 6 December 2005 / Published online: 4 January 2006

Abstract Irrigation scheduling requires an operational means to quantify plant water stress. Remote sensing may offer quick measurements with regional coverage that cannot be achieved by current ground-based sampling techniques. This study explored the relation between variability in fine-resolution measurements of canopy temperature and crop water stress in cotton fields in Central Arizona, USA. By using both measurements and simulation models, this analysis compared the standard deviation of the canopy temperature (σ_{T_c}) to the more complex and data intensive crop water stress index (CWSI). For low water stress, field σ_{T_c} was used to quantify water deficit with some confidence. For moderately stressed crops, the σ_{T_c} was very sensitive to variations in plant water stress and had a linear relation with field-scale CWSI. For highly stressed crops, the estimation of water stress from σ_{T_c} is not recommended. For all applications of σ_{T_c}, one must account for variations in irrigation uniformity, field root zone water holding capacity, meteorological conditions and spatial resolution of T_c data. These sensitivities limit the operational application of σ_{T_c} for irrigation scheduling. On the other hand, σ_{T_c} was most sensitive to water stress in the range in which most irrigation decisions are made, thus, with some consideration of daily meteorological conditions, σ_{T_c} could provide a relative measure of temporal variations in root zone water availability. For large irrigation districts, this may be an economical option for minimizing water use and maximizing crop yield.

Communicated by P. Waller

M. P. González-Dugo (✉)
CIFA Alameda del Obispo, IFAPA, Apdo 3092,
14080 Córdoba, Spain
E-mail: mariap.gonzalez.ext@juntadeandalucia.es
Tel.: +34-957-016030
Fax: +34-957-016043

M. S. Moran · R. Bryant
USDA ARS Southwest Watershed Research Center,
Tucson, AZ, USA

L. Mateos
Instituto de Agricultura Sostenible, CSIC, Apdo 4084,
14080 Córdoba, Spain

Introduction

Irrigation is a significant means of raising production in agricultural crops. It is essential in arid environments, and is often used to increase crop productivity in semi-arid and humid areas. Because of the increasing demand of water for general purposes, the supply available for irrigation is decreasing and irrigation costs are rising. As a result, new management strategies have been proposed based on controlled deficit irrigation to ensure low water loss with minimum yield reduction. To achieve this delicate balance between water use and crop yield, farm managers need an operational means to quantify plant water stress and thus optimize their irrigation scheduling.

Classical methods for monitoring crop water stress include in situ measurements of soil water content, plant properties, or meteorological variables to estimate the amount of water lost from the plant-soil system during a given period. These methods are time consuming and produce point information that give poor indications of the overall status of the field concerned (Jackson 1982), unless very large numbers of samples are processed. However, with the advances in radiometry and remote sensing, it may be possible to extend such plant-based methods to the field scale. For example, direct measurement of leaf temperature has been related to crop water stress based on the fact that under stress free conditions, the water transpired by the plants evaporates and cools the leaves. Conversely, in a water deficit situation, little water is transpired and leaf temperature increases. This is also the dominant mechanism when the canopy is considered as a whole (Idso and Baker 1967).

This theory has been used to develop spectral indices that combine meteorological data with remotely sensed information to provide a relative measure of plant water status and health. The crop water stress index (CWSI) (Idso et al. 1981; Jackson et al. 1981), based on the difference between canopy and air temperatures, was a significant advance in this respect. The CWSI has been commonly applied to the detection of water stress of plants, but difficulties in measuring canopy temperature of crops with less than 100% vegetation cover has limited its operational application. The water deficit index (WDI) (Moran et al. 1994) offered a means to overcome this limitation by combining spectral vegetation indices with composite surface temperature, based on the same theory as CWSI, to estimate water deficit for partially-vegetated fields.[1]

Even though these indices have shown important benefits for farm management, the input requirements for computation (particularly meteorological data recorded in situ at the time of the overpass) have been a constraint for more general use by farmers. An alternative approach would be to exploit the facts that crops do not show water stress until they deplete the readily available water in the root zone and that water stress amongst individual plants inevitably varies due to variations in factors such as soil properties, rooting depth and irrigation application. Therefore, spatial variability in the canopy temperature should be very low in the absence of water stress, but should increase as the level of water stress increases. The readily available water is defined as the fraction of the available water holding capacity in the root zone (difference between the water content at field capacity and wilting point) that a crop can extract without reduction of its transpiration. A common assumption is that the transpiration reduction is linearly related to the depletion below the readily available water (Ritchie 1973; Doorembos and Pruitt 1977; Allen et al. 1998). The readily available water fraction is often adjusted to account for the effect of the evaporative demand on the transpiration rate.

There are two main reasons that water stress does not occur simultaneously in all the spots of an irrigated field. Firstly, soil water properties in general and soil water storage in particular vary significantly across any field (Nielsen et al. 1973). Secondly, all the irrigation methods have an inherent non-uniformity that can be enhanced by poor design and/or management (Clemmens and Dedrick 1994). Thus, the water available to be extracted by the crop after an irrigation, at a given time and location in the field, is the minimum between the root zone available water holding capacity and, in the absence of rainfall, the irrigation water infiltrated at that location. As the soil dries, the crop plants will begin to show signs of water stress that vary spatially depending on water availability at their respective locations. The plants with low available water will have reduced transpiration and higher canopy temperatures earlier than plants with more available water. Therefore, the standard deviation of canopy temperature is likely to increase as the field-averaged crop stress increases with the number of days after an irrigation event.

The use of the standard deviation of canopy temperature (σ_{T_c}), as an indicator of water stress may have notable advantages. First, compared to conventional ground-based methods for determining field-scale crop stress, measurement cost and time would likely be reduced. Second, compared to CWSI and WDI, image processing requirements would be greatly reduced since systematic errors in the measurement of spatially distributed canopy temperature would have little or no effect on its standard deviation, thus sensor calibration and atmospheric correction would not be necessary. Finally, complementary ground-based meteorological measurements would not be required. A notable disadvantage of this approach is similar to one of the drawbacks of CWSI, i.e., both methods are based on canopy temperature, not composite temperature. Thus, the measurement of composite temperature from an airborne sensor must be made when the crop's vegetation cover is nearly 100%.

Measurement of this stress-related variability was investigated in early works by Clawson and Blad (1982) and Gardner et al. (1981), then revisited by Bryant and Moran (1999) and Gonzalez-Dugo et al. (2000). However, little progress has been made towards quantifying the complex relationship between canopy temperature variability, water stress and the spatial pattern of water availability, particularly the likelihood that the variability in canopy temperature will increase with the stress severity. Also, little attention has been given to situations of severe water stress in which transpiration in the field will be greatly reduced, starting at locations with less available water. The canopy temperature variability should then decrease after a certain level of stress has been exceeded. Greater understanding of these interactions would clearly be beneficial for irrigation scheduling.

With recent improvements in accuracy, deployment and spatial resolution of thermal sensors, the use of the variability of remotely sensed canopy temperature deserves further exploration. This study uses both measurements and models to explore the hypothesis that water stress variability varies with field-scale water stress. The limits for application of σ_{T_c} as an indicator of water stress were analyzed under different available water uniformity patterns and under different environmental conditions.

[1] At this point in the discussion, it is important to define three measures of surface temperature: T_c, T_o and T_s. T_c is the canopy temperature, defined by Norman et al. (1995) as the temperature at which the "vegetation dominates the (measurement) field of view minimizing the effect of soil". T_o is the temperature of the soil surface. T_s is the surface composite temperature, defined by Norman et al. (1995) as the "aggregate temperature of all objects comprising the surface", which was shown by Kustas et al. (1990) to be a linear function of T_c and T_o. When the surface is completely covered by vegetation, $T_s = T_c$ and when the surface is bare soil, $T_s = T_o$.

Simulation

A simple water budget model was used to simulate root zone water depletion between irrigations. This was combined with basic CWSI energy balance theory to determine the canopy temperature variability associated with daily water loss. The scope of the combined model is the quantitative formulation of our hypothesis. Therefore, it should not be used as a predictive or operational tool. The theory and application of this simulation is described here.

Theory

The water budget in the root zone for a period between two consecutive irrigations, assuming no rainfall or drainage, can be simplified to:

$$D_i = D_{i-1} + E_i, \tag{1}$$

where D_i and D_{i-1} (mm) are the root zone available water depletion on days i and $i-1$, respectively, and E_i (mm) is crop evaporation on day i. With full ground cover, crop evaporation can be assumed to be equal to transpiration. Then, the crop evaporation-water depletion function is calculated as:

$$\left(1 - \frac{E_i}{E_{ix}}\right) = 0 \quad \text{if } D_i < D_a, \tag{2a}$$

$$\left(1 - \frac{E_i}{E_{ix}}\right) = \frac{D_i - D_a}{D_r - D_a} \quad \text{if } D_i \geqslant D_a, \tag{2b}$$

where E_i and E_{ix} (mm) are, respectively, actual and maximum crop evaporation on day i, D_a is the readily available depth of water in the root zone (mm) and D_r (mm) is the root zone available water holding capacity.

The energy balance equation can be expressed as:

$$R_n - G = \lambda E + H, \tag{3}$$

where R_n, G, λE and H (W m^{-2}) are net radiation, soil heat flux, latent heat flux and sensible heat flux, respectively. The sensible heat flux can be expressed in terms of temperature difference as:

$$H = \rho C_p \frac{T_c - T_a}{r_a}, \tag{4}$$

where ρ (kg m^{-3}) is the air density, C_p (J kg^{-1} °C^{-1}) the specific heat of the air, r_a (s m^{-1}) the aerodynamic resistance, and T_c and T_a (°C) the canopy temperature and air temperature at the reference height, respectively.

The CWSI is expressed as:

$$\text{CWSI} = \frac{(T_c - T_a) - (T_c - T_a)_{ll}}{(T_c - T_a)_{ul} - (T_c - T_a)_{ll}}, \tag{5}$$

where the subscripts ll and ul refer to lower (well-watered crop) and upper (non-transpiring crop) limits, respectively.

Substituting Eq. 4 into Eq. 3 and solving for

$$T_c - T_a = \frac{r_a}{\rho C_p}[(R_n - G) - \lambda E]. \tag{6}$$

In a well-watered crop, λE is equal to the potential crop evaporation (expressed in g m^{-2} s^{-1}) times the latent heat of vaporization (λ, J g^{-1}). In a completely stressed crop, λE is zero, thus (6) reduces to:

$$(T_c - T_a)_{ul} = \frac{r_a(R_n - G)}{\rho C_p}. \tag{7}$$

Between both extremes λE is calculated by multiplying the potential crop evaporation by the fraction E_i/E_{ix} obtained from Eq. 2.

Application

The water budget and energy balance models were combined and applied to a soil with an available water holding capacity of 125 mm m^{-1} and a crop with a root depth of 1.6 m. Thus, D_r was 125 mm m^{-1}×1.6 m = 200 mm. The readily available water in the root zone was 0.6×D_r, i.e., 120 mm. It was assumed that vegetation cover was 100% (thus all latent heat flux was from crop transpiration), $(R_n - G) = 620$ W m^{-2}, $T_a = 35.8$°C, $r_a = 14.1$ s m^{-1}, and λE from a well-watered crop was equal to −700 W m^{-2}; values that represent typical environmental conditions during the measurements described in the next section. When the crop experienced water stress, it was assumed that the instantaneous latent heat flux at the measuring time was reduced at the same rate as the daily transpiration calculated from Eq. 2. Potential crop evaporation was assumed 9 mm day^{-1}, a typical value for cotton in the simulation environment.

If the irrigation strategy is to achieve high application efficiency, then a significant part of the field should be below field capacity after the irrigation. Contrarily, if the target depth seeks avoiding water deficit, then after irrigation the whole field will be at field capacity. But neither field capacity nor available water holding capacity is constant across the field. On the other hand, if the irrigation does not fill the whole field to field capacity, then both irrigation non-uniformity and variability of D_r will determine the variability of the available water after the irrigation. Therefore, in both cases, it can be considered that the root zone available water after the irrigation is randomly distributed. We assumed five different coefficients of variation (CV): CV equal to 0.40, 0.30, 0.20, 0.10, and 0.01. These CV values should cover the range of field uniformities for the different irrigation methods and, presumably, the range of root zone available water holding capacities. Two hundred values of just-after-irrigation available water were then randomly generated assuming a normal frequency distribution, taking into account findings that some soil hydrologic properties (Vieira et al. 1981) and irrigation

uniformity test data [i.e., Bralts and Kesner (1983) for drip irrigation, Hart and Reynolds (1965) for sprinkler irrigation, and Oyonarte and Mateos (2003) for furrow irrigation] usually form bell-shaped distributions. Actual crop transpiration, the reduction of crop transpiration relative to that of a well watered crop, T_c and CWSI were calculated with the combined model along a 26-day drying cycle for each of the 200 virtual field locations. The sensitivity of σ_{T_c} to changes in environmental conditions was studied by varying r_a, λE or R_n in the energy balance-CWSI model while keeping the other two (λE and R_n, r_a and R_n, r_a and λE, respectively) constant.

Experimental methods

The data used for this analysis were obtained from the NASA Airborne Terrestrial Application Sensor (ATLAS) over the University of Arizona Maricopa Agricultural Center (MAC), southwest of Phoenix, Arizona. The collaboration between the USDA-ARS and the NASA Stennis Space Center to investigate the use of ATLAS spectral imagery for farm management applications produced a set of six flights during the cotton and sorghum growing seasons, from April to September 1998. The sensor specifications for these flights were: 2.5 m data resolution, a spectral range from 0.45 to 12.2 μm divided into 14 channels, and flightline overlap of nearly 75%. The ground support was provided by USDA personnel, including crop and GPS surveys, radiometric target deployment, and field radiometer and spectrometer measurements. A detailed field survey was conducted during each overpass to record such data as crop height, surface moisture, soil roughness and tillage direction, together with comments on important information or anomalies.

Reference tarps were deployed to provide targets of known reflectance for calibration of the airborne data (Moran et al. 2001). Four surface areas, each of 16×16 m^2, were covered with tarps of four different reflectances (0.04, 0.08, 0.48, and 0.64). This was an area equivalent to 6×6 ATLAS pixels, and an area of 2×2 pixels was considered to be unaffected by the edges and suitable as a calibration reference. Additional measurements of surface temperature of the tarps were made with an infrared thermometer during every overpass to calibrate the thermal bands. Field radiometry over two targets in the visible/near-infrared spectra complemented the reflectance information of the tarps. These targets were a field of alfalfa with high vegetation coverage and a large packed-earth landing strip. A calibrated reference $BaSO_4$ plate was used to convert the radiance measurements to reflectance (Jackson et al. 1987).

The images were calibrated to at-sensor radiance by on-board instruments, and reflectance and temperature were retrieved from the ATLAS bands using a linear relation computed using the tarps and field radiometry targets. The slopes and intercepts were obtained for each band and flight with all the regression coefficients over 0.99. Values of the soil adjusted vegetation index (SAVI) were computed from surface reflectance, as

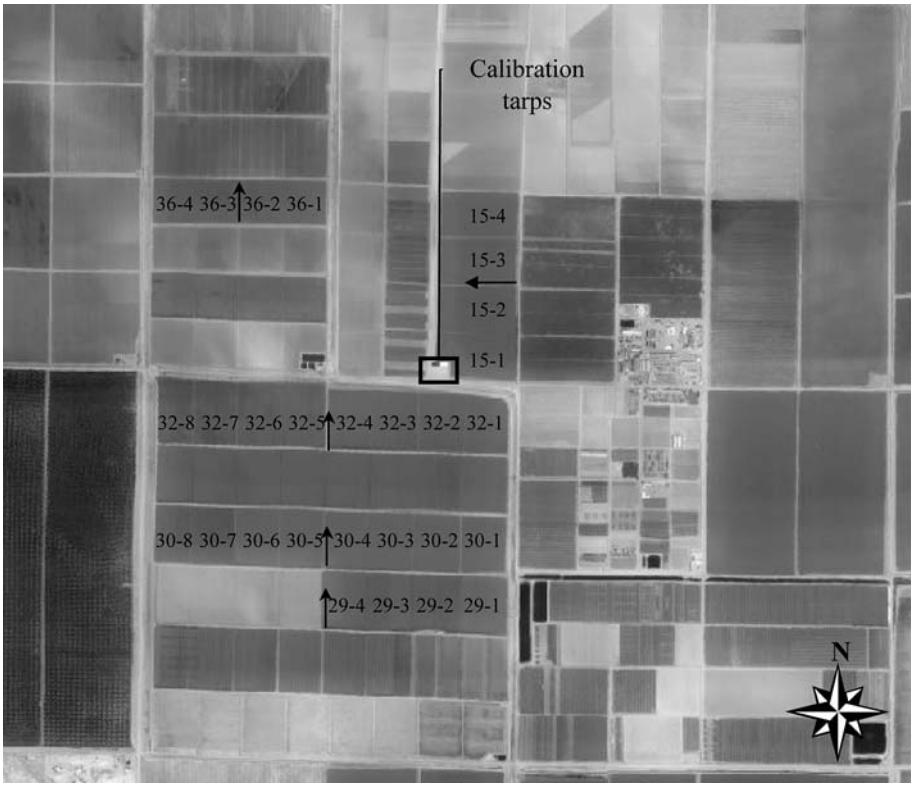

Fig. 1 ATLAS image of Maricopa Agricultural Center, taken on 17 September 1998 (day of year 260). *Labels* indicate the reference number of the selected fields and the *arrows* indicate the direction of the furrows

$$\mathrm{SAVI} = \frac{(\rho_{\mathrm{NIR}} - \rho_{\mathrm{red}})}{(\rho_{\mathrm{NIR}} + \rho_{\mathrm{red}} + L)}(1 + L), \tag{8}$$

where ρ_{NIR} and ρ_{red} are reflectance factors in the near-infrared and red spectra, respectively, and L is a soil normalization factor generally considered to be 0.5 (Huete 1988).

The analysis presented here was restricted to furrow-irrigated cotton crops. The selection of cotton fields was limited by two main factors: crop stage and image quality.

To ensure that the cotton crop had reached maturity, only data obtained during the last three flights (on days of the year, DOY, 193, 231, and 260) were used. Furthermore, based on field survey information, it was determined that a SAVI = 0.5 corresponded to a vegetation cover of 75%. So, only those fields with SAVI greater than 0.5 were included in the analysis of the relation between σ_{T_c} and CWSI. To ensure high image quality and avoid bidirectional effects, only flightlines containing the reference tarps were selected and, within these images, only fields with less than 10° viewing angle were chosen. With these constraints, a total of 56 field/images (20, 20, and 16 for DOY 193, 231, and 260, respectively), with areas ranging from 0.5 to 1.4 ha, were chosen (Fig. 1). All the fields were extracted from calibrated images, discarding three to four pixels from the field boundaries to avoid edge effect.

Measurements started at 10:20 solar time, but most of the selected field/images were measured after 11:00, when the differences in temperature between stressed and non-stressed crops are most readily detected (Gardner et al. 1981). Since meteorological data over the crop were not available, the required data at the time of every flightline were retrieved from the AZMET meteorological station at MAC.

The CWSI was computed for the 56 field/images using Eq. 5, obtaining $(T_c - T_a)$ by subtracting the AZMET air temperature from the mean T_c extracted from the image. The lower and upper limits (subscripts ll and ul, respectively), for the canopy minus air temperature were calculated developing Eq. 6 as in Jackson et al. (1981):

$$(T_c - T_a)_{(\mathrm{ll,ul})} = \frac{r_a(R_n - G)}{\rho C_p} \frac{\gamma\left(1 + \frac{r_{c(ll,ul)}}{r_a}\right)}{\Delta + \gamma\left(1 + \frac{r_{c(ll,ul)}}{r_a}\right)} - \frac{\mathrm{VPD}}{\Delta + \gamma\left(1 + \frac{r_{c(ll,ul)}}{r_a}\right)}, \tag{9}$$

where $r_{c(ll,ul)}$ (s m^{-1}) is the canopy resistance for a full-cover well-watered crop (subscript ll) or for a full-cover non-transpiring crop (subscript ul), Δ (kPa °C^{-1}) is the slope of the saturated vapor pressure–temperature relation, VPD is the vapor pressure deficit of the air, γ (kPa °C^{-1}) is the psychrometric constant, and all other variables have been defined above.

R_n was calculated as the sum of the incoming and outgoing flux densities, using the equations described by Brutsaert (1982, Sect. 6.1). The short-wave radiation was obtained from measured solar radiation and cotton albedo equal to 0.21 (Monteith and Unsworth 1990, Sect. 6). The upward and downward long-wave radiations were derived from the surface and air temperatures, respectively. Cotton long-wave emissivity was adopted equal to 0.96 (Monteith and Unsworth 1990, Sect. 6) and the atmospheric emissivity was calculated using the equation proposed by Idso and Jackson (1969). The aerodynamic resistance was computed using a semi-empirical equation proposed by Thom and Oliver (1977) and recommended by Jackson et al. (1988) for its ability to obtain realistic results under both high and low windspeed conditions:

$$r_a = 4.72\frac{[\ln(z - d/z_o)]^2}{1 + 0.54u}, \tag{10}$$

where z (m) is the measurement height, d (m) the zero-plane displacement height, z_o (m) the roughness length, and u (m s^{-1}) the windspeed. Values of z_o and d were derived from field measured plant height [h (m)] as $z_o = 0.13h$ and $d = 0.67h$.

Note that Eq. 9 is equivalent to Eq. 7 when $r_{c,ul} \to \infty$. For the analysis of the measured data, we assumed $r_{c,ul} = 500$ s m^{-1}, a large resistance compared to $r_{c,ll}$. The canopy resistance at potential transpiration ($r_{c,ll}$) was determined for each of the three measuring days by adjusting its value until the lowest CWSI value on that day was zero. This method was used by Jackson et al. (1981) to assess the canopy resistance of a wheat crop after an irrigation. The calibration of $r_{c,ll}$ was based on the assumption that at least one of the fields selected each measuring day was transpiring at potential rate. An alternative criterion was making zero the average CWSI of the 10% of the fields with the lowest CWSI. The results were slightly different, revealing a weakness of the analysis. The values of $r_{c,ll}$ adjusted following the first criterion were 41, 42, and 16 s m^{-1} for DOY 193, 231, and 260, respectively.

Results and discussion

According to the combined model, as water stress increased, σ_{T_c} rose until it reached a peak value (Fig. 2). The peak σ_{T_c} occurred at CWSI values decreasing with the uniformity of the water availability. For instance, σ_{T_c} was maximal at CWSI values of 0.20 and 0.38 when the CV of the water availability were 0.1 and 0.2, respectively. The σ_{T_c} then decreased with further rises in average CWSI. Therefore, the same standard deviation corresponded to different levels of water stress, and the relationship between σ_{T_c} and CWSI varied depending on the irrigation/soil uniformity.

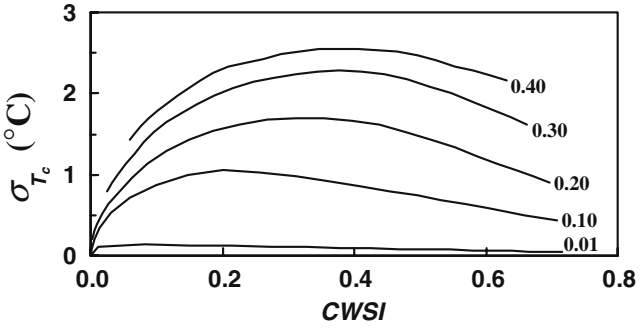

Fig. 2 Standard deviation of the canopy temperature (σ_{T_c}) versus field-scale crop water stress index (*CWSI*) simulated for five different levels of variability of the root zone water availability (indicated by their respective coefficients of variation)

The measurements of σ_{T_c} and CWSI for crops with greater than 75% cover (SAVI > 0.5) by the ATLAS sensor led to the same general conclusions (Fig. 3). For well-watered cotton (CWSI < 0.1), the measurements of σ_{T_c} tended to cluster in an undifferentiated fashion with values averaging 0.63°C (Fig. 3). On day 193, when the fields showed stress values of 0.1 < CWSI < 0.3, σ_{T_c} increased linearly with CWSI. Modeled results for a surface of CV = 0.15 showed the same increasing trend for this interval (Fig. 3), although following a different trajectory. As all the plants started to experience stress (CWSI > 0.3), values of modeled σ_{T_c} decreased slightly with CWSI (Fig. 3). The same trend could be observed in the measured σ_{T_c}, although the limited number of fields (six) in this situation prevented confirming this pattern. This result agreed with observations by Clawson and Blad (1982) for corn, with temperature variablity leveling off as stress became increasingly severe.

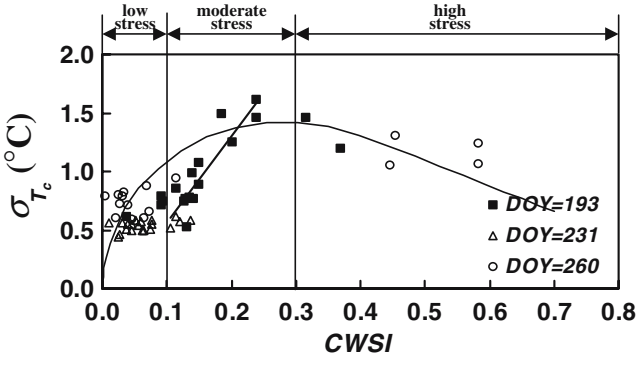

Fig. 3 Standard deviation of the canopy temperature (σ_{T_c}) versus field-scale crop water stress index (*CWSI*) for three measuring days (12 July, 19 August, and 17 September 1998, days of year, DOY, 193, 231, and 260, respectively) in cotton fields of the Maricopa Research Center. The linear regression in the moderate stress band follows the equation $\sigma_{T_c} = 7.40\,\mathrm{CWSI} - 0.18$ ($r^2 = 0.77$). The *curve* represents simulated variations using the combined water budget and energy balance model for a coefficient of variation of the root zone water availability equal to 0.15

For intermediate levels of water stress, the σ_{T_c} ranged from about 0.6 to 1.6°C. The lower limit of this interval was within the range of 0.3–0.7°C, found by Gardner et al. (1981) and Clawson and Blad (1982) as the onset of plant stress and representing the need for irrigation. It is also notable that the biggest increase in σ_{T_c} was associated with CWSI values from 0.1 to 0.3. This corresponds well with the suggested CWSI threshold value for irrigation scheduling, CWSI = 0.2 (Reginato 1983), and suggests that the σ_{T_c} could be an indicator for cotton irrigation scheduling. For the conditions of this experiment, a value of σ_{T_c} close to 0.7°C, corresponding to a CWSI equal to 0.15, seemed to be the threshold value for triggering irrigation. Since MAC is a well-managed production farm, it is not surprising that 50 of the 56 cotton field/images selected for this study had CWSI values less than 0.3.

Therefore, both the combined model and the ATLAS measurements supported the hypothesis that the relationship between canopy temperature variability and water stress severity depends on the spatial pattern of water availability, which is strongly dependent on the irrigation strategy. If the applied irrigation water filled the root zone at all the locations in the field, the relationship between canopy temperature variability and the stress severity would be largely determined by the variability of the root zone water holding capacity. However, with a deficit irrigation strategy, the irrigation uniformity would be the main determinant of this relationship. In an intermediate situation, both irrigation uniformity and root zone available water holding capacity would influence the relationship.

It is well known that the amount of water infiltrated along irrigation furrows varies from head to tail. The infiltration opportunity time in the upper part of open-end furrows is greater than in their downstream part. Therefore, it could be hypothesized that crop water deficits, and thus increases in T_c, would appear near the tail of the furrows earlier and with more intensity than near their head. If so, the difference in head–tail T_c $\left(T_c^{\mathrm{head}} - T_c^{\mathrm{tail}}\right)$ would be an indicator of stress. However, our data did not support this hypothesis. Contrary to expectations, $T_c^{\mathrm{head}} - T_c^{\mathrm{tail}}$ had a weak but statistically significant ($P < 0.01$) positive correlation with the field-scale CWSI (Fig. 4). A lack of correlation could have indicated that the irrigation depth usually applied in MAC is greater than that necessary to replenish the soil along the entire length of the furrows. However, the positive correlation is more difficult to explain, although it could be related to a head–tail gradient of soil water holding capacity caused by the repetitive practice of furrow irrigation. In summary, Fig. 4 leads to the conclusion that the variability of water availability detected with our data (σ_{T_c}) was due to soil variation rather than to irrigation non-uniformity.

Coming back to the potential of σ_{T_c} as a crop water stress indicator, there are at least two issues that need to be explored: first, the effect of varying environmental conditions on the relationship between σ_{T_c} and crop

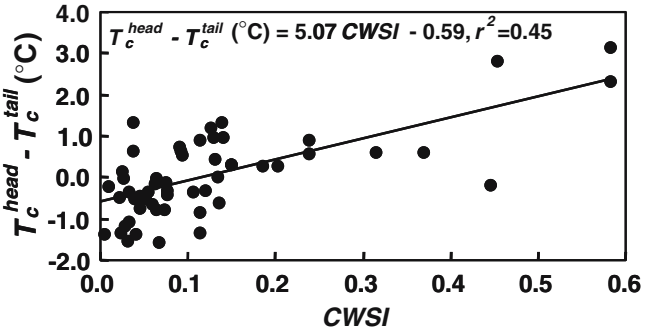

Fig. 4 Relationship and linear regression between the head and tail canopy temperature difference $\left(T_c^{head} - T_c^{tail}\right)$ and the field-scale crop water stress index (*CWSI*) for fields with moderate stress. T_c^{head} and T_c^{tail} were obtained by averaging T_c of 30-m (12 pixels) wide strips along the upper (*head*) and lower (*tail*) side of the field, respectively

water stress and, second, the spatial resolution of the T_c measurements required to determine crop water stress with sufficient precision. The first issue was explored with the combined model, being aware of its limitations (e.g., the water balance does not consider variations of the evaporation rate with changes in the evaporative demand). The model indicated that decreasing r_a or λE yielded increasing σ_{T_c} for equal CWSI and that σ_{T_c} was insensitive to changes in R_n (noted that changes in R_n affect the terms in the numerator and denominator of Eq. 5 equally). Nevertheless, the sensitivity of the model to environmental conditions seemed to be excessive since the measured data yielded smaller variations of σ_{T_c} with variations of r_a in the same range tested with the model. Therefore, this issue requires further research. Regarding the second issue, temperature variability is scale dependent, decreasing as the grid size increases. Therefore, the possibility of applying this approach using remote sensors with less spatial resolution than the 2.5-m provided by the ATLAS sensor is restricted.

In order to evaluate the scale effect, the ATLAS pixels were aggregated to simulate different grid sizes (5, 10, 20, 30, 60, and 90 m). Figure 5 shows the σ_{T_c} versus CWSI coefficient of determination (r^2) under moderate water stress for different grid sizes. The coefficient of determination decreased from 0.77 (for the ATLAS grid size) to 0.40 (for 60 m and greater grid sizes). The weak correlation for spatial resolution less than 10 m reduces the applicability of σ_{T_c} for the detection of crop water stress when satellite sensors like Landsat−7, with a spatial resolution in the thermal band of not less than 60 m, are used.

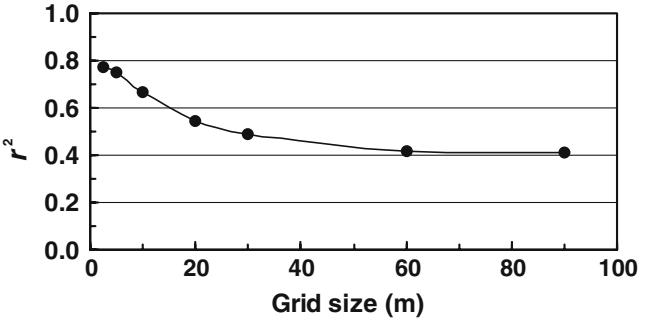

Fig. 5 Change of the σ_{T_c} versus CWSI relationship regression coefficient (r^2) with increasing grid size

Conclusions

Remote sensing of canopy temperature by airborne scanners with fine spatial resolution provides information and coverage that cannot be acquired with conventional sampling. This study explored the use of within-field variations in canopy temperature (σ_{T_c}) to determine field-scale plant water stress. Such a simple method can be easily and quickly computed and can provide instantaneous information on field water status with little ancillary data.

Based both on measurements and modeling, this analysis provided many insights into the application of σ_{T_c} for determining crop water stress. For low water stress, field σ_{T_c} is relatively small. For moderately stressed crops, σ_{T_c} was very sensitive to variations in plant water stress and had a linear relation with field-scale CWSI. However, care must be taken if the empirical relationship used to relate water stress to σ_{T_c} was obtained in a field with a different degree of uniformity of the root zone water availability to that of the field under evaluation. For high water stress, the estimation of water stress from σ_{T_c} was poor and does not seem recommendable. The σ_{T_c} may have potential for application to irrigation scheduling since it was most sensitive to water stress in the range in which most irrigation decisions are made ($0.1 < \text{CWSI} < 0.3$; $0.5°\text{C} < \sigma_{T_c} < 1.5°$ C). For large irrigation districts, this may be an economical option for minimizing water use and maximizing crop yield. However, in order for the precision to be sufficient for practical applications, the scanner must have sufficient spatial resolution. The minimum resolution in our case appeared to be about 10 m.

Acknowledgements This research was made possible with funding and support provided by NASA Stennis Space Center. Additional support was provided through the Cooperative Research Program of the Organisation for Economic Cooperation and Development (OECD). The authors would like to thank the staff at the University of Arizona Maricopa Agricultural Center and pilot Larry Hinton for their research support and collaboration.

References

Allen RG, Pereira LS, Raes D, Smith M (1998) Crop evapotranspiration. Guidelines for computing crop water requirements. FAO irrigation and drainage paper no 56. FAO, Rome

Bralts VF, Kesner CD (1983) Drip irrigation field uniformity estimation. Trans ASAE 26:1369–1374

Brutsaert W (1982) Evaporation into the atmosphere theory, history and applications. D Reidel Publishing Company, Dordrecht

Bryant RB, Moran MS (1999) Determining crop water stress from crop canopy temperature variability. In: Proceedings of the international airborne remote sensing conference, Ottawa, Ontario, Canada, 21–24 June 1999, pp I289–I296

Clawson KL, Blad BL (1982) Infrared thermometry for scheduling irrigation of corn. Agron J 74:311–316

Clemmens AJ, Dedrick AR (1994) Irrigation techniques and evaluations. In: Tanji KK, Yaron B (eds) Adv Series Agric Sci, vol 22. Springer, Berlin Heidelberg New York, pp 64–103

Doorembos J, Pruitt WO (1977) Crop water requirements. FAO irrigation and drainage paper no.24. FAO, Rome

Gardner BR, Blad BL, Watts DG (1981) Plant and air temperature in differentially-irrigated corn. Agric Meteorol 25:207–217

González-Dugo MP, Bryant RB, Moran MS (2000) Uso de la variabilidad térmica en la determinación del estrés hídrico en cultivos (in Spanish). In: Proceedings of XVIII Congreso Nacional de Riegos, Huelva, Spain, 20–22 June 2000

Hart WE, Reynolds WN (1965) Analytical design of sprinkler systems. Trans ASAE 8:83–85, 89

Huete AR (1988) A soil-adjusted vegetation index (SAVI). Remote Sens Environ 25:295–309

Idso SB, Baker DG (1967) Relative importance of reradiation, convection and transpiration in heat transfer from plants. Plant Physiol 42:631–640

Idso SB, Jackson RD (1969) Thermal radiation from the atmosphere. J Geophys Res 74:5397–5403

Idso SB, Jackson RD, Pinter PJ Jr, Reginato RJ, Hatfield JL (1981) Normalizing the stress-degree-day parameter for environmental variability. Agric Meteorol 24:45–55

Jackson RD (1982) Canopy temperature and crop water stress. Adv Irrig 1:43–85

Jackson RD, Idso SB, Reginato RJ, Pinter PJ (1981) Canopy temperature as a crop water stress indicator. Water Resour Res 17:1133–1138

Jackson RD, Moran MS, Slater PN, Biggar SF (1987) Field calibration of reference reflectance panels. Remote Sens Environ 22:145–158

Jackson RD, Kustas WP, Choudhury BJ (1988) A reexamination of the crop water stress index. Irrig Sci 9:309–317

Kustas WP, Choudhury BJ, Inoue Y, Pinter PJ Jr, Moran MS, Jackson RD, Reginato RJ (1990) Ground and aircraft infrared observations over a partially-vegetated area. Int J Remote Sens 11:409–427

Monteith JL, Unsworth MH (1990) Principles of environmental physics, 2nd edn. Edward Arnold, London

Moran MS, Clarke TR, Inoue Y, Vidal A (1994) Estimating crop water deficit using the relation between surface-air temperature and spectral vegetation index. Remote Sens Environ 49:246–263

Moran MS, Bryant RB, Clarke TR, Qi J (2001) Deployment and calibration of reference reflectance tarps for use with airborne cameras. Photog Eng Remote Sens 67:273–286

Nielsen DR, Biggar JW, Erh KT (1973) Spatial variability of field-measured soil-water properties. Hilgardia 42:215–260

Norman JM, Divakarla M, Goel NS (1995) Algorithms for extracting information from remote thermal-IR observations of the earth's surface. Remote Sens Environ 51:157–168

Oyonarte NA, Mateos L (2003) Accounting for soil variability in the evaluation of furrow irrigation. Trans ASAE 45:85–94

Reginato RJ (1983) Field quantification of crop water stress. Trans ASAE 26:772–775

Ritchie JT (1973) Influence of soil water status and meteorological conditions on evaporation from a corn canopy. Agron J 65:893–897

Thom AS, Oliver HR (1977) On Penman's equation for estimating regional evaporation. Q J R Meteorol Soc 103:345–357

Vieira SR, Nielsen DR, Biggar JW (1981) Spatial variability of field-measured infiltration rate. Soil Sci Soc Am J 45:1040–1048